Journal of Process Control 32 (2015) 109–116

Contents lists available at ScienceDirect

Journal of Process Control

journal homepage: www.elsevier.com/locate/jprocont

Canonical variate analysis-based monitoring of process correlation structure using causal feature representation

Benben Jiang [a,b], Xiaoxiang Zhu [b], Dexian Huang [a], Richard D. Braatz [b,*]

[a] Department of Automation, Tsinghua University and Tsinghua National Laboratory for Information Science and Technology, Beijing 100084, China
[b] Department of Chemical Engineering, Massachusetts Institute of Technology, Cambridge, MA 02139, USA

ARTICLE INFO

Article history:
Received 3 February 2015
Received in revised form 21 May 2015
Accepted 26 May 2015
Available online 17 June 2015

Keywords:
Fault monitoring
Correlation structural fault
Causal map
Dimensionality reduction technique
Canonical variate analysis

ABSTRACT

Although the monitoring of process variables has been extensively studied, techniques for monitoring faults in the process correlation structures have not yet been fully investigated. The typical methods based on the covariance matrix of the process data for process monitoring have limited capability to effectively monitor underlying structural changes. This paper proposes a canonical variate analysis (CVA) approach based on the feature representation of causal dependency (CD) for the monitoring of faults associated with changes in process structures, which employs CD for pretreating the data and subsequently utilizes CVA for quantifying dissimilarity. Apart from the improved performance of capturing the underlying connective structure information, the utilization of the CD feature in the first step provides more application-dependent representations compared with the original data, as well as decreased degree of redundancy in the feature space by incorporating causal information. The effectiveness of the proposed CD-based approach for the monitoring of structural changes is demonstrated for both single faults and multiple faults in simulation studies of a networked system. In the simulation results, the CD-based method performs the best, followed by correlation-based and then variable-based methods.

1. Introduction

As manufacturing facilities become increasingly integrated and large scale, the potential for faults to dynamically propagate in non-intuitive ways to produce significant harm to equipment, life, and the environment has increased. The rapid detection of faults and associated identification of their causes are, therefore, of outmost importance, which has attracted the interest of many researchers and practitioners. However, most of the process monitoring methods developed so far, including the multivariate statistical control chart approaches [1–3], dimensionality reduction techniques [4–8], and time-series or state-space methods [9,10], focus on the monitoring of process variable faults [11,12].

Compared with the achievements in the monitoring of process variable faults, limited exploration has been done on the important complementary problem of monitoring the faults of process correlation structures [13]. With the emerging big data concept, the monitoring of correlation structures has become of increased interest [14]. The explosive growth of process data along with the increasingly large-scale industries provides a valuable resource for the analysis and operations of industrial processes. This paper aims to develop a new approach for monitoring changes in the process structure.

Typical approaches adopted for monitoring the process correlations are based on the process information described by the covariance matrix. Example approaches include the generalized variance [15,16,18], the conditional entropy [17], and the likelihood ratio test (LRT) [19,20]. The covariance-based methods experience inherent limitations in the detection of local anomalies as well as the subsequent identification of the fault origins. In other words, the inherent structure of the process is not explicitly taken into account in the covariance-based methods. For instance, two variables, x and y, can be connected in several different ways such as (i) direct connection $x \to y$, (ii) indirect connection $x \to z \to y$ or (iii) co-regulated by a third variable z ($z \to x$ and $z \to y$). In all these cases, the variability between x and y may be similar, and a deviation on their underlying causal relationship may pass undetected and undiscerned by only monitoring the covariance. In order to access and use the underlying information of the process correlation structure, alternative measures of structural relationships should be adopted in the process monitoring procedures.

An efficient way to explore the relationship for the underlying structure amongst variables is using causal information. A

* Corresponding author at: 77 Massachusetts Avenue, Room E19-551, Cambridge, MA 02139, USA. Tel.: +1 617 253 3112; fax: +1 617 258 0546.
E-mail address: braatz@mit.edu (R.D. Braatz).

http://dx.doi.org/10.1016/j.jprocont.2015.05.004
0959-1524/

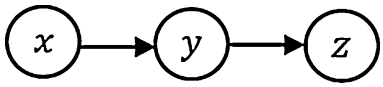

Fig. 1. Causal linkage of the variables x, y, and z.

causal map can clearly reflect the directional linkages between any two variables. In addition, the information of causal connectivity can be used to reduce the correlated degree for the feature space of correlation, thereby enhancing the performance of fault monitoring. It was shown in [21] that the monitoring performance was more sensitive in a space of uncorrelated features. For example, in Fig. 1, without considering the causal connectivity among the three variables, the feature representation of correlation contains three components, i.e., $r_{x,y}$, $r_{y,z}$, and $r_{x,z}$. From the causal links in Fig. 1, $r_{x,z}$ is redundant with ($r_{x,y}$, $r_{y,z}$). In other words, the inclusion of $r_{x,z}$ in the feature representation of correlation does not provide more information but increases the degree of correlation.

It is important to note that the directional connectivity of the components within the plant can play a significant role in fault monitoring [22–24]. Several papers describe the construction of the causal map from a process flow diagram or piping and instrumentation diagram [23,25,40]. Their results showed that data-driven techniques in combination with cause-and-effect relationships among process variables can lead to efficient monitoring of faults. The linkage of data-driven analysis with a causal relationship of the process has been identified as a promising approach to fault monitoring [22,23,25].

Previously, the authors introduced a feature representation of causal dependency (CD) to incorporate the data-driven techniques in conjunction with the causal information [26–28]. The CD is utilized to quantify the similarity between the relationship of two causally related variables under current operating conditions and historical operating conditions. It was reported in [29] that better fault monitoring results are achieved for features that are more application-dependent. In terms of application-dependence in process facilities, the CD is an appropriate feature to represent deviations in the process structure. In this article, an approach based on the CD feature representation is proposed for the monitoring of process structural faults. The proposed CD-based approach can potentially facilitate to detect process structural faults and to identify the root causes, owing to the finer description of the underlying structure and the less correlated feature space of the CD by utilizing causal information. Different from the previous work [27] and [28] which focused on the monitoring of *process variable faults*, this article investigates the monitoring of *process correlation structures*. In addition, this work incorporates a dimensionality reduction step based on Canonical Variate Analysis (CVA), which generates dynamic state-space models from the process data to improve the monitoring proficiency.

The rest of this paper is organized as follows. Section 2 briefly reviews the traditional CVA-based data-driven monitoring method. Section 3 describes the CD-based approach for monitoring process structural faults. The effectiveness of the proposed method is demonstrated by a gene network system in Section 4. Section 5 summarizes the conclusions.

2. Canonical variate analysis

The Canonical Variate Analysis (CVA) method, which serves as the technique in the step of dissimilarity quantification, is briefly reviewed in this section. More details of CVA can be found in [30,31].

2.1. CVA theorem

CVA is a dimensionality reduction technique in multivariate statistical analysis which maximizes the correlation between two selected sets of variables. Consider vectors of process variables $\boldsymbol{x} \in R^m$ and $\boldsymbol{y} \in R^n$ with covariance matrices $\Sigma_{\boldsymbol{xx}}$ and $\Sigma_{\boldsymbol{yy}}$ and cross-covariance matrix $\Sigma_{\boldsymbol{xy}}$. The orthogonal basis is chosen as those linear combinations of a variable set $\boldsymbol{x}$ that are more correlated with the linear combinations of another variable set $\boldsymbol{y}$ in the CVA approach, where these linear combinations are named *canonical variables* and are represented as $\boldsymbol{c}$ and $\boldsymbol{d}$, namely

$$\boldsymbol{c} = \boldsymbol{J}\boldsymbol{x} \tag{1}$$

$$\boldsymbol{d} = \boldsymbol{L}\boldsymbol{y} \tag{2}$$

where $\boldsymbol{J}$ and $\boldsymbol{L}$ are projection matrices that can be calculated by solving the SVD [31]:

$$\Sigma_{\boldsymbol{xx}}^{-1/2}\Sigma_{\boldsymbol{xy}}\Sigma_{\boldsymbol{yy}}^{-1/2} = \boldsymbol{U}\Sigma\boldsymbol{V}^{\mathrm{T}} \tag{3}$$

where Σ is the diagonal matrix of nonnegative singular values in descending order, and $\boldsymbol{U}$ and $\boldsymbol{V}$ are matrices of the right and left singular vectors. Then the projection matrices $\boldsymbol{J}$ and $\boldsymbol{L}$ are obtained by

$$\boldsymbol{J} = \boldsymbol{U}^{\mathrm{T}}\Sigma_{\boldsymbol{xx}}^{-1/2} \tag{4}$$

$$\boldsymbol{L} = \boldsymbol{V}^{\mathrm{T}}\Sigma_{\boldsymbol{yy}}^{-1/2} \tag{5}$$

The matrices $\boldsymbol{U}^{\mathrm{T}}$ and $\boldsymbol{V}^{\mathrm{T}}$ guarantee that the canonical variables are only pairwise correlated, and the matrices $\Sigma_{\boldsymbol{xx}}^{-1/2}$ and $\Sigma_{\boldsymbol{yy}}^{-1/2}$ scale the canonical variables so that $\boldsymbol{c}$ and $\boldsymbol{d}$ have unit variance.

2.2. CVA algorithm

Hotelling initially proposed the CVA concept for multivariate statistical analysis, which was not employed to system identification until Akaike's work on ARMA models [30]. The CVA method was further developed for identifying state-space models by Larimore [30]. Given time series output data $\boldsymbol{y}(t) \in R^{m_y}$ and input data $\boldsymbol{u}(t) \in R^{m_u}$, the linear state-space model is given by

$$\boldsymbol{x}(t+1) = \boldsymbol{A}\boldsymbol{x}(t) + \boldsymbol{B}\boldsymbol{u}(t) + \boldsymbol{v}(t) \tag{6}$$

$$\boldsymbol{y}(t) = \boldsymbol{C}\boldsymbol{x}(t) + \boldsymbol{D}\boldsymbol{u}(t) + \boldsymbol{E}\boldsymbol{v}(t) + \boldsymbol{w}(t) \tag{7}$$

where $\boldsymbol{x}(t)$ is a state vector, $\boldsymbol{v}(t)$ and $\boldsymbol{w}(t)$ are independent white noise processes, and $\boldsymbol{A}$, $\boldsymbol{B}$, $\boldsymbol{C}$, $\boldsymbol{D}$ and $\boldsymbol{E}$ are coefficient matrices.

Important to the CVA algorithm is the concept of past and future vectors. At a particular time instant $t \in (1, \cdots, n)$, the past vector $\boldsymbol{p}(t)$ containing the past outputs and inputs is

$$\boldsymbol{p}(t) = \left[\boldsymbol{y}^{\mathrm{T}}(t-1), \boldsymbol{y}^{\mathrm{T}}(t-2), \cdots, \boldsymbol{y}^{\mathrm{T}}(t-l), \boldsymbol{u}^{\mathrm{T}}(t-1), \boldsymbol{u}^{\mathrm{T}}(t-2), \cdots, \boldsymbol{u}^{\mathrm{T}}(t-l)\right]^{\mathrm{T}} \tag{8}$$

and the future vector $\boldsymbol{f}(t)$ comprising of the outputs in the present and future is

$$\boldsymbol{f}(t) = \left[\boldsymbol{y}^{\mathrm{T}}(t), \boldsymbol{y}^{\mathrm{T}}(t+1), \cdots, \boldsymbol{y}^{\mathrm{T}}(t+h)\right]^{\mathrm{T}} \tag{9}$$

where l and h are the numbers of lags in vectors $\boldsymbol{p}(t)$ and $\boldsymbol{f}(t)$, respectively.

By substituting the matrix $\Sigma_{\boldsymbol{xy}}$ with Σ_{pf}, $\Sigma_{\boldsymbol{xx}}$ with $\Sigma_{\boldsymbol{pp}}$, and $\Sigma_{\boldsymbol{yy}}$ with $\Sigma_{\boldsymbol{ff}}$, the matrices $\boldsymbol{J}$, $\boldsymbol{L}$, and $\boldsymbol{D}$ can be calculated via the SVD as (3). The states $\boldsymbol{x}(t)$ in (6) and (7) can be obtained from the data using the CVA states as

$$\boldsymbol{x}_d(t) = \boldsymbol{J}_d\boldsymbol{p}(t) = \boldsymbol{U}_d^{\mathrm{T}}\widehat{\Sigma}_{\boldsymbol{pp}}^{-1/2}\boldsymbol{p}(t) \tag{10}$$

where $\boldsymbol{J}_d = \boldsymbol{U}_d^{\mathrm{T}}\widehat{\Sigma}_{\boldsymbol{pp}}^{-1/2}$ and $\boldsymbol{U}_d$ contains the first d columns of $\boldsymbol{U}$ in (3) [31].

The numbers of lags l and h and the state order d is not known in advance, which can be determined by the lags and the order that minimize the Akaike information criterion [31].

2.3. Process monitoring measures

In the CVA method, two types of statistics T_s and T_r are computed from the process model in normal operating conditions (NOC), which are defined as

$$T_s(t) = \boldsymbol{x}_d^{\mathrm{T}}(t)\boldsymbol{x}_d(t) \tag{11}$$

and

$$T_r(t) = \boldsymbol{x}_e^{\mathrm{T}}(t)\boldsymbol{x}_e(t) \tag{12}$$

where

$$x_e(t) = \boldsymbol{J}_e\boldsymbol{p}(t) = \boldsymbol{U}_e^{\mathrm{T}}\widehat{\Sigma}_{\boldsymbol{pp}}^{-1/2}\boldsymbol{p}(t) \tag{13}$$

and $\boldsymbol{U}_e$ contains the last $e = l(m_u + m_y) - d$ columns of $\boldsymbol{U}$ in (3) [31,32].

The T_s statistic measures the variations inside the canonical states, while the T_r statistic measures the variations in the residuals.

3. The proposed causal dependence-based approach for monitoring process structural faults

3.1. Feature representation of causal dependence

Feature representation, which is a step that generates derived values (features) from an initial set of data to facilitate the desired task, is crucial for fault monitoring. Sarfraz et al. [29] reported that better fault monitoring results are achieved for features that are more application-dependent. In terms of application-dependence of the feature generation, features that measure the linkages between process variables (e.g., correlation coefficient) are more appropriate than features directly using the process variables themselves for the monitoring of process correlation structures.

In addition, the performance of process monitoring is reported to be more sensitive in a space of uncorrelated features [21]. In other words, less redundancy in the feature space results in better process monitoring results. Noticeably, the cause-and-effect relationships among process variables can be used to reduce the degree of correlation in the feature representation. In the example of Fig. 1, monitoring based on traditional correlation features require the correlation between every two variables ($r_{x,y}$, $r_{y,z}$, and $r_{x,z}$), even though the correlation coefficient $r_{x,z}$ is redundant with the correlation coefficients ($r_{x,y}$, $r_{y,z}$). Such redundancy can be avoided by incorporating the information on the causal connectivity among the variables.

In this regard, Chiang and Braatz [26,27] proposed a feature representation that incorporates multivariate statistics with causal information, named the *Causal Dependence* (CD), to detect deviations in the relationship between causally related variables. The basic idea of the CD-based feature measures for process structural changes is that the causal dependencies (CDs) under abnormal conditions show some deviation from the distribution of the CDs under normal conditions. In the CD-based feature representation, the process behavior is measured by the CDs instead of by the process variables themselves.

The CD, which is derived based on the multivariate T^2 statistic, is used to quantify the similarity between the relationship of two causally related variables under current operating conditions and historical operating conditions. When the CD is larger than the predefined threshold, the causal dependency of the two variables is violated. The CD requires a causal map containing the causal relationship between all of the measured variables, which can be derived either by a *priori* knowledge of the process or by the techniques of causality, as for example [33].

To formally define the causal dependency, let c refer to the cause variable and e as the effect variable. The CD is based on the multivariable T^2 statistic, which is defined by

$$\mathrm{CD}_{c,e} = T_{c,e}^2 = (\boldsymbol{y} - \bar{\boldsymbol{y}})^{\mathrm{T}}\boldsymbol{S}_{c,e}^{-1}(\boldsymbol{y} - \bar{\boldsymbol{y}}) \tag{14}$$

where $\boldsymbol{y} = [c \quad e]^{\mathrm{T}}$, $\bar{\boldsymbol{y}}$ is the mean of $\boldsymbol{y}$, and $\boldsymbol{S}_{c,e}$ is the sample covariance for variables c and e. Based on the training data under NOC, the mean of the variable $\bar{\boldsymbol{y}} = [\bar{c} \quad \bar{e}]^{\mathrm{T}}$ and the sample covariance $\boldsymbol{S}_{c,e}$ are computed for each causal dependency.

For the example in Fig. 1, only two components ($\mathrm{CD}_{x,y}$ and $\mathrm{CD}_{y,z}$) are required in the feature representation of the CD. According to the application-dependent and uncorrelated aspects of the feature representations, the CD-based feature is expected to perform the best for the monitoring of process structures, followed by the correlation-based and then the variable-based features (which is demonstrated for case studies in Section 4).

Remark 1. The CD feature can be extended to handle serial correlations in the data by augmenting the observation vectors with time lags, i.e., $\boldsymbol{y} = \begin{bmatrix} c(t) & c(t+1) & \cdots \\ e(t) & e(t+1) & \cdots \end{bmatrix}$.

Remark 2. The feature representation of the CD is computationally efficient for the feature generation step, compared to the correlation feature representation, especially when the number of process variables n is very large. This difference in computational cost is a result of the typically high number of correlation coefficients calculated in the latter ($n(n-1)/2$, for every pairing of two variables), while only the coefficient calculations between the causally related variables are required for the CD.

3.2. Dissimilarity quantification and fault detection

Once the calculation of CDs for normal conditions (training data) is completed in (14), quantification of dissimilarity among the CDs is performed, as well as the determination of thresholds for normal operating limits. Distance- or angle-based metrics are typically utilized for the dissimilarity quantification [34]. The distance-based metrics are more often encountered for fault detection methods, including the principal component analysis (PCA)-, partial least-squares (PLS)-, and CVA-based methods.

This article uses the CVA method to assess the dissimilarity among the CDs obtained from normal operating data. In other words, CVA is performed on the training CDs to determine the upper control limits. Two detection indices termed as D_s and D_r, similar to the CVA's T_s and T_r ((11) and (12)) respectively, are defined as

$$D_s(t) = \boldsymbol{x}_d^{\mathrm{T}}(t)\boldsymbol{x}_d(t) \tag{15}$$

and

$$D_r(t) = \boldsymbol{x}_e^{\mathrm{T}}(t)\boldsymbol{x}_e(t) \tag{16}$$

where the past vector $\boldsymbol{p}(t)$ and the future vector $\boldsymbol{f}(t)$ are

$$\boldsymbol{p}(t) = \left[\boldsymbol{CD}^{\mathrm{T}}(t-1), \boldsymbol{CD}^{\mathrm{T}}(t-2), \cdots\right]^T \tag{17}$$

and

$$\boldsymbol{f}(t) = \left[\boldsymbol{CD}^{\mathrm{T}}(t), \boldsymbol{CD}^{\mathrm{T}}(t+1), \cdots\right]^T \tag{18}$$

The correlation structures of the process is considered normal if the dissimilarity statistics are below the thresholds, i.e., $D_s \le T_\alpha^2$ and $D_r \le \delta_\alpha^2$, where T_α^2 and δ_α^2 denote the upper control limits for the dissimilarity index in the canonical states and residuals with a significance level α, respectively. CVA is one way to determine

Table 1
Definition of the faults and respective variables involved for correlation structures. δ is a multiplicative factor that changes the model parameters ($\delta = 1$ for NOC).

Fault	Correlation structure changed
GN1	$u_1 \to x_1\ (x_1(t) = 1.2\delta(u_1(t) + 0.60u_1(t-1) + 0.30u_1(t-2)) + 0.8u_2(t) + v_1(t))$
GN2	$\begin{cases} u_1 \to y_6 \\ x_1 \to x_2 \end{cases} \left(\begin{cases} y_6(t) = 1 + 0.40\delta(u_1(t) + 0.60u_1(t-1) - 0.30u_1(t-2)) + v_8(t) \\ x_2(t) = 0.05 + 0.22\delta(x_1(t) - 0.40x_1(t-1) - 0.20x_1(t-2)) + v_3(t) \end{cases} \right)$

the dissimilarities among different samples; other approaches can be utilized to derive distance-based or angle-based similarity statistics.

Similar to the standard PCA and CVA method, the CDs generated from the training and testing data are first normalized before the SVD is implemented. Additionally, T_α^2 and δ_α^2 in the CD context can be derived in two ways. One way is the analytical method that computes the thresholds based on assumed Gaussian distributions [35]. The other way is the empirical approach based on the calibration samples under NOC [32,36]. For instance, a 99% confidence upper control limit can be obtained as the D_s or D_r value below which 99% of the calibration data are located. This article uses the latter method to determine the upper control limits.

4. Case studies for a gene network

In this section, a gene network is used to evaluate the proposed CD-based approach for the monitoring of process structural faults, in comparison with correlation-based (i.e., perform CVA on the correlation coefficients where the two statistics that measure the variations inside the canonical states, and the residuals are termed as C_s and C_r, respectively) and variable-based (i.e., directly perform CVA on the process variables where the two statistics are termed as T_s and T_r) methods. In each case study, the normal data set for training contains 2500 observations; and the testing data set for each fault also consists of 2500 observations. Each faulty data set started with no faults, and the faults were triggered after the 1000th observation into the run. The data have a sampling time of one second.

The proposed CD-based approach for the monitoring of process structural faults is evaluated for a gene network adapted from [37], which is composed by 16 nodes (or variables) causally related according to the description provided in Fig. 2.

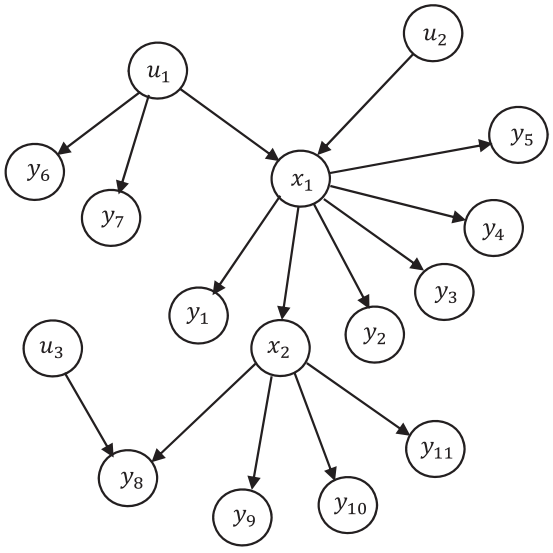

Fig. 2. Causal description of a gene network [37].

In the case studies, the original variable relationships are linearized according to

$$\begin{cases} x_1(t) = 1.2(u_1(t) + 0.60u_1(t-1) + 0.30u_1(t-2)) + 0.8u_2(t) + v_1(t) \\ y_1(t) = 0.60(x_1(t) + 0.50x_1(t-1) + 0.20x_1(t-2)) + v_2(t) \\ x_2(t) = 0.05 + 0.22(x_1(t) - 0.40x_1(t-1) - 0.20x_1(t-2)) + v_3(t) \\ y_2(t) = 1 + 0.40(x_1(t) - 0.20x_1(t-1) - 0.10x_1(t-2)) + v_4(t) \\ y_3(t) = 0.062 + 0.16(x_1(t) + 0.40x_1(t-1) + 0.60x_1(t-2)) + v_5(t) \\ y_4(t) = 0.60(x_1(t) + 0.80x_1(t-1) + 0.10x_1(t-2)) + v_6(t) \\ y_5(t) = 0.70(x_1(t) + 0.40x_1(t-1) + 0.20x_1(t-2)) + v_7(t) \\ y_6(t) = 1 + 0.40(u_1(t) + 0.60u_1(t-1) - 0.30u_1(t-2)) + v_8(t) \\ y_7(t) = 0.56 + 0.15(u_1(t) + 0.40u_1(t-1) + 0.60u_1(t-2)) + v_9(t) \\ y_8(t) = 0.80(u_3(t) + 0.60u_3(t-1) + 0.30u_3(t-2)) + 0.51x_2(t) + v_{10}(t) \\ y_9(t) = 1.30(x_2(t) + 0.50x_2(t-1) + 0.50x_2(t-2)) + v_{11}(t) \\ y_{10}(t) = 1 + 0.40(x_2(t) + 0.40x_2(t) + 0.60x_2(t)) + v_{12}(t) \\ y_{11}(t) = 0.028 + 1.30(x_2(t) + 0.60x_2(t) - 0.30x_2(t)) + v_{13}(t) \end{cases} \quad (19)$$

where u_1, u_2, and u_3 are the input variables, x_1 and x_2 are the states, and the rest are outputs. Each v_i is a white-noise sequence with a signal-to-noise ratio of 10%. The system was subject to the two faults (see Table 1), where Fault GN1 is a single fault and Fault GN2 is a multiple fault. The statistics for detecting a single fault are directly applicable for detecting multiple faults since the thresholds for (15) and (16) depend only on the data from the normal operating conditions. For the faults, δ denotes a multiplicative factor that causes a change in a model parameter.

4.1. Single-fault case study

A single fault (Fault GN1) is examined in this scenario, which occurs in the process structure from input variable u_1 to state variable x_1. In order to provide a sound comparative assessment of the detection performances, the false alarm rates are maintained at the same level ($\alpha = 1\%$) for comparing the missed detection rates in different circumstances throughout this study. The same procedure was repeated 1000 times in order to estimate the confidence levels of the missed detection rates at different fault magnitudes. The mean missed detection rate as a function of the fault magnitude δ for Fault GN1 by using the CD-based, correlation-based, and variable-based methods are plotted in Fig. 3.

As the fault magnitude increases, the mean missed detection rate decreases in all of the methods. Moreover, the mean missed detection rate in all three methods approach zero as the fault magnitude increases, indicating the enhanced detectability for large faults. In addition, the gap in the missed detection rates between the CD-based and correlation-based methods enlarges as the magnitude of fault increases from 1.1 to 1.5, while the gap between the CD-based and variable-based methods enlarges as fault magnitude increases from 1.1 to 1.8.

For the same fault magnitude δ, the performance of fault detection using the correlation-based method always outperformed that using the variable-based method (Fig. 3), which confirms that the correlation-based feature representation was more appropriate for the monitoring of the correlation structural faults than variable-based feature representation. In addition, the CD-based

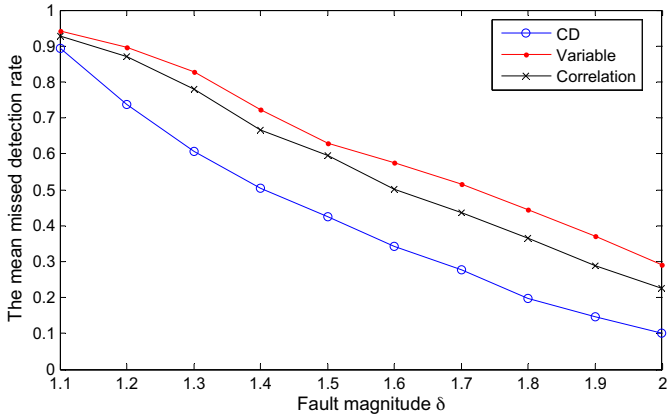

Fig. 3. The mean missed detection rate as a function of the fault magnitude for Fault GN1 ($\delta = 1$ under NOC). The methods in the legend are: CD (i.e., perform CVA on the CDs), correlation (i.e., perform CVA on the correlation coefficients), and Variable (i.e., directly perform CVA on the process variables) methods. For each method, a fault was indicated if either the state or residual statistic violated threshold.

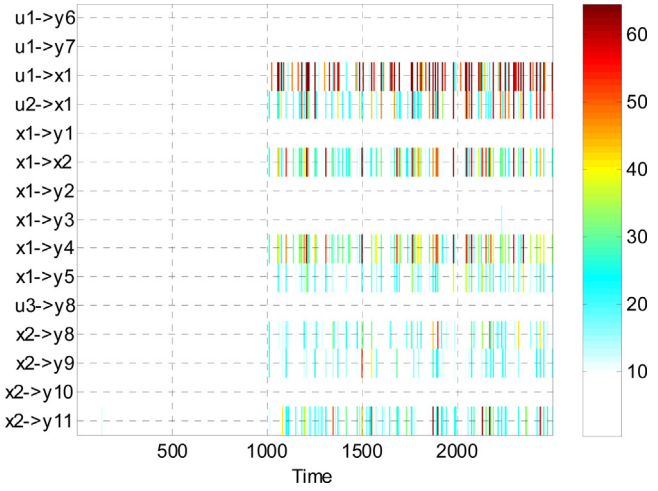

Fig. 4. CVA-based contributions for Fault GN1 with fault magnitude $\delta = 1.5$.

method always performed better than both the correlation-based and variable-based methods for the same fault magnitude δ. For example, at the fault magnitude $\delta = 1.6$, the missed detection rates of the CD-based algorithm is 34.4%, compared to 50.1% to the correlation-based algorithm, which is more than a factor of 1.4 improved detection for the CD-based method. Compared to the variable-based algorithm, the mean missed detection rate for the CD-based algorithm is nearly a factor of 1.7 lower (34.4% vs. 57.6%). The main reasons for the superior performance of the CD-based approach are that (i) the CD-based feature representation can effectively capture the changes in the process correlation structures (the application-dependent aspect); and (ii) the lower redundancy of the CD-based feature representation leads to the improved monitoring performance by incorporating the causal information.

Overall, the results are consistent with the above discussions that the CD-based feature performs the best for the monitoring of process structural faults, followed by the correlation-based, and then the variable-based features.

Once a fault has been detected, a propagation path of faulty correlations can be derived by using causal linkages. Such information plays an important role in the determination of the root cause of abnormal events.

Contribution plots [31] are the commonly used technique for determining which components are most likely related to the statistics no longer being within normal operation (aka "faulty correlation"). Here the CVA-based contributions [38] are utilized to identify the faulty correlations of Fault GN1. The contribution plot of the structural change with the case of fault's magnitude $\delta = 1.5$ is displayed in Fig. 4 as a color map [39], which indicates that correlations $u_1 \to x_1$, $u_2 \to x_1$, $x_1 \to x_2$, $x_1 \to y_4$, $x_1 \to y_5$, $x_2 \to y_8$, $x_2 \to y_9$, and $x_2 \to y_{11}$ are faulty for Fault GN1. Further, considering the directional links among these faulty correlations, a propagation path of faulty correlations for Fault GN1 can be obtained, as shown in Fig. 5. Fig. 5 indicates that the faulty correlation $u_1 \to x_1$ and/or $u_2 \to x_1$ are associated with the source of the propagation path and are most strongly associated with the origin of Fault GN1. This identification is accurate, as Fault GN1 is associated with a change in the correlation $u_1 \to x_1$ (Table 1).

4.2. Multiple faults case study

Multiple faults of correlation structures occurring at the same time are likely to happen for many industrial processes. For instance, this situation can be caused by a change in a physical coefficient that affects at least two different correlations. The task of identifying multiple faults is rather challenging. A multiple fault (Fault GN2) in the gene network system is used to further investigate the performance of the proposed approach for monitoring structural changes in this part. Fault GN2 occurs in the correlations of $u_1 \to y_6$ and $x_1 \to x_2$. The mean missed detection rate as a function of the fault magnitude δ for Fault GN2 by using the CD-based, correlation-based, and variable-based methods are plotted in Fig. 6.

Again, as the fault magnitude δ increases, the mean missed detection rate decreases in all of the methods (Fig. 6). The mean missed detection rates in all three methods also approach zero as the fault magnitude increases, indicating the improved detectability for larger faults. The mean missed detection rate is sensitive to the fault magnitude for small to intermediate values of δ, with the fault magnitude of highest sensitivity dependent on the method.

For the same fault magnitude δ, the CD-based algorithm performs the best for the monitoring of Fault GN2, followed by the correlation-based and then the variable-based algorithms (Fig. 6). At the fault magnitude $\delta = 1.3$, the mean missed detection rate for the CD-based algorithm is more than a factor of 2.5 lower (31.3% vs. 81.1%) than for the variable-based algorithm, and nearly a factor of 2.3 for the correlation-based algorithm (31.3% vs. 74.5%).

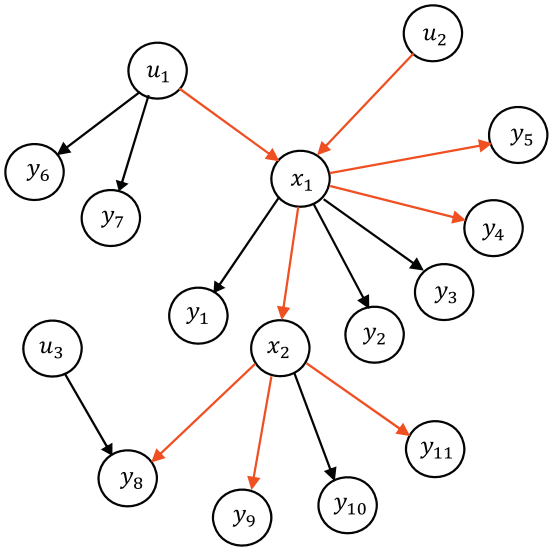

Fig. 5. A propagation path of faulty correlations for Fault GN1 (faulty correlations are shown as vectors between nodes with red color).

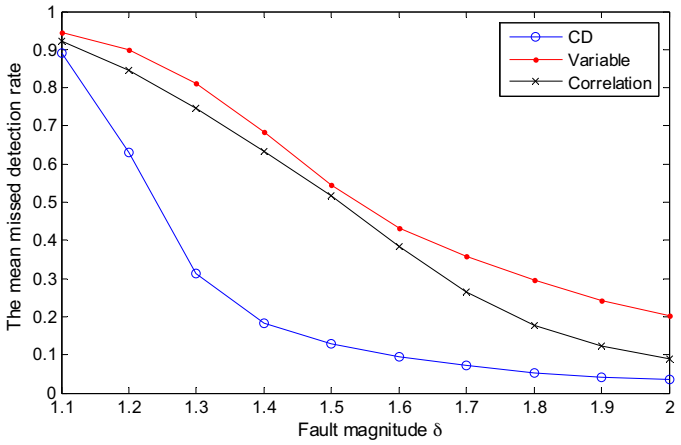

Fig. 6. The mean missed detection rate as a function of the fault magnitude for Fault GN2 ($\delta = 1$ under NOC). The methods in the legend are: CD (i.e., perform CVA on the CDs), correlation (i.e., perform CVA on the correlation coefficients), and Variable (i.e., directly perform CVA on the process variables) methods. For each method, a fault was indicated if either the state or residual statistic violated threshold.

The main reasons are similar as discussed above, which are that (i) the deviations in the process correlation structures can be effectively captured by the CD-based feature representation; and (ii) the improved monitoring performance results from the less redundancy of the CD-based feature representation by incorporating causal information.

The objective of fault detection is to be *sensitive* enough to detect all possible faults, while being *robust* to data that are independent of the training set. The sensitivity was quantified by the mean missed detection rate (aka type II error [31,32]) for faults in the testing set. The robustness was quantified by the false alarm rate (type I error [31,32]) for the testing set under NOC. The extent to which the methods (with statistics D_s, D_r, C_s, C_r, T_s, and T_r) are sensitive to Fault GN2 is displayed in Fig. 7 with the type I error maintained at the same level ($\alpha = 1\%$) in all methods to enable a fair comparison of the type II errors. Both the state and residual statistics D_s, D_r for the CD method much more persistently indicate a fault compared to the other methods.

The contributions of the structural changes with the fault magnitude of $\delta = 1.5$ for Fault GN2 are plotted in Fig. 8. The faulty correlations are $u_1 \to y_6, x_1 \to x_2, x_2 \to y_8, x_2 \to y_9$, and $x_2 \to y_{11}$. The propagation paths of faulty correlations for Fault GN2 are displayed in Fig. 9, which indicates that there are two separate propagation paths, i.e., $u_1 \to y_6$ and $x_1 \to x_2 \to y_8 (x_2 \to y_9, x_2 \to y_{11})$. Fig. 8 indicates that Fault GN2 corresponds to multiple faults, with the faulty correlations $u_1 \to y_6$ and $x_1 \to x_2$ being the sources of the two propagation paths, that is, are most likely related to the root causes of Fault GN2. The faulty correlations $u_1 \to y_6$ and $x_1 \to x_2$ indicate that the structural faults occur in the relationships between variable u_1 and variable y_6 and between variable x_1 and variable x_2:

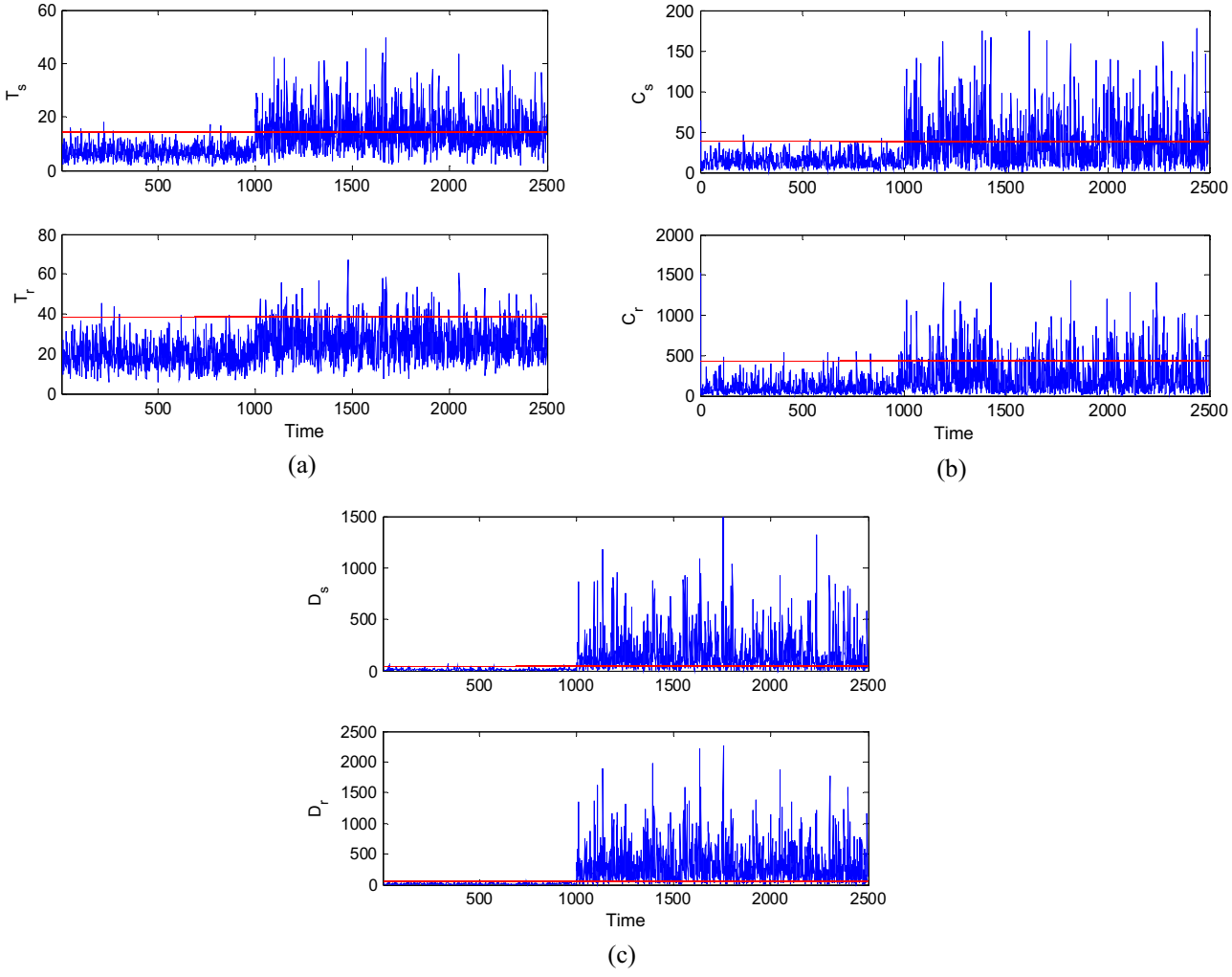

Fig. 7. Multivariate statistics for the detection for Fault GN2 with the fault magnitude $\delta = 1.6$ for (a) variable-based, (b) correlation-based, and (c) CD-based methods.

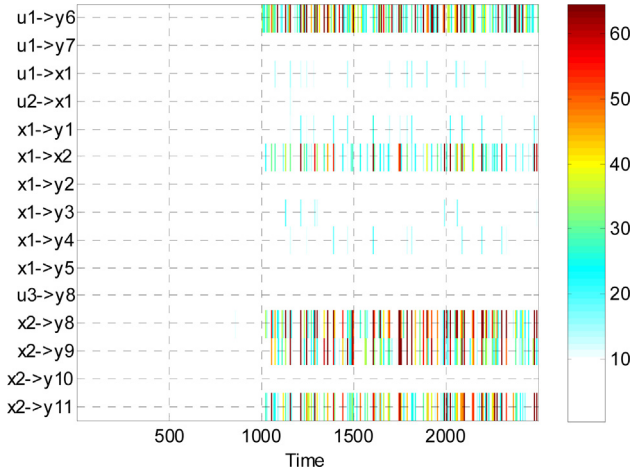

Fig. 8. CVA-based contributions for Fault GN2 with fault magnitude $\delta = 1.5$.

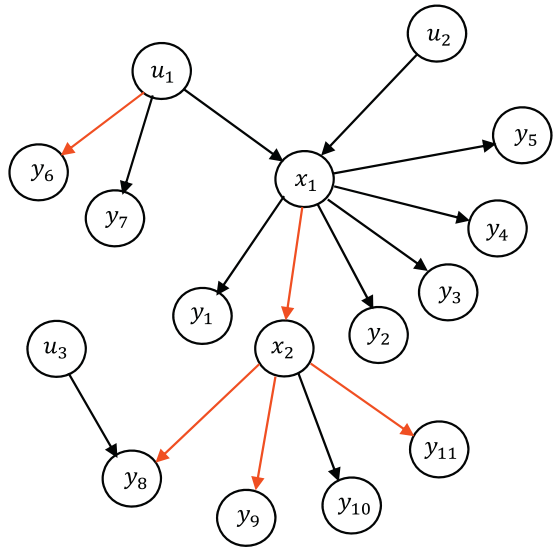

Fig. 9. A propagation path of faulty correlations for Fault GN2 (faulty correlations are shown as vectors between nodes with red color). (For interpretation of the references to color in this figure legend, the reader is referred to the web version of this article.)

the proposed approach identified the correct causes of Fault GN2 (Table 1).

The results demonstrate effectiveness of the proposed CD-based approach not only for identifying the case of single faults but also for multiple faults.

5. Conclusions

This article presents a causal dependency (CD)-based approach for the monitoring of process correlation structures. Two steps are involved in the proposed monitoring approach: (1) the generation of CD features and (2) dissimilarity quantification. The first step provides means to construct application-dependent and uncorrelated features that facilitate the subsequent step for quantifying similarity or dissimilarity. In addition to handling the underlying connective structure information in the data, the CD-based approach can also bring the benefits for detecting process structural faults and for identifying the origins of such structural changes, owing to the less correlated feature space of the CDs by incorporating causal information. The simulation results demonstrate effectiveness of the proposed CD-based method for the cases of both single faults and multiple faults for a gene network model. The proposed approach also applies to systems with material and energy recycles and feedback control loops. The causal map is sufficiently general to handle these more complicated relationships between variables, with the causal dependencies and canonical variate analysis computed the same way as described in the article

Acknowledgements

This work is supported by the National Basic Research Program of China (2012CB720505) and the National Natural Science Foundation of China (21276137). The first author is grateful for the financial support from China Scholarship Council.

References

[1] W.A. Shewhart, Economic Control of Quality of Manufactured Product, D. Van Nostrand Company, Inc., New York, 1931.
[2] H. Hotelling, The generalization of student's ratio, Ann. Math Stat. 2 (1931) 360–378.
[3] R.B. Crosier, Multivariate generalizations of cumulative sum quality-control schemes, Technometrics 30 (1988) 291–303.
[4] A. Raich, A. Cinar, Statistical process monitoring and disturbance diagnosis in multivariable continuous processes, AIChE J. 42 (1996) 995–1009.
[5] J.F. MacGregor, C. Jaechle, C. Kiparissides, M. Koutoudi, Process monitoring and diagnosis by multiblock PLS methods, AIChE J. 40 (1994) 826–838.
[6] B.M. Wise, N.B. Gallagher, The process chemometrics approach to process monitoring and fault detection, J. Process Control. 6 (1996) 329–348.
[7] W. Li, H.H. Yue, S. Valle-Cervantes, S.J. Qin, Recursive PCA for adaptive process monitoring, J. Process Control 10 (2000) 471–486.
[8] W. Ku, R.H. Storer, C. Georgakis, Disturbance detection and isolation by dynamic principal component analysis, Chemom. Intell. Lab. Syst. 30 (1995) 179–196.
[9] A. Negiz, A. Çinar, PLS, balanced, and canonical variate realization techniques for identifying VARMA models in state space, Chemom. Intell. Lab. Syst. 38 (1997) 209–221.
[10] A. Negiz, A. Çinar, Statistical monitoring of multivariable dynamic processes with state-space models, AIChE J. 43 (1997) 2002–2020.
[11] B. Abbasi, S. Niaki, M. Abdollahian, S. Hosseinifard, A transformation based multivariate chart to monitor process dispersion, Int. J. Adv. Manuf. Technol. 44 (2009) 748–756.
[12] V.B. Ghute, D.T. Shirke, A multivariate synthetic control chart for process dispersion, Qual. Technol. Quant. Manag. 5 (2008) 271–288.
[13] L. Liu, J. Zhong, Y. Ma, A multivariate synthetic control chart for monitoring covariance matrix based on conditional entropy, in: E. Qi, J. Shen, R. Dou (Eds.), Proceedings of the 19th International Conference on Industrial Engineering and Engineering Management, Springer, Berlin/Heidelberg, 2013, pp. 99–107.
[14] V. Mayer-Schonberger, K. Cukier, Big Data: A Revolution That Will Transform How We Live, Work, and Think, John Murray Publishers, London, 2013.
[15] M.A. Djauhari, Improved monitoring of multivariate process variability, J. Qual. Technol. 37 (2005) 32–39.
[16] F.B. Alt, Multivariate quality control, in: N.L. Johnson, S. Kotz, C.R. Read (Eds.), The Encyclopedia of Statistical Sciences, Wiley, New York, 1984, pp. 110–122.
[17] J.L. Guerrero-Cusumano, Testing variability in multivariate quality control: a conditional entropy measure approach, Inf. Sci. 86 (1995) 179–202.
[18] M.A. Djauhari, M. Mashuri, D.E. Herwindiati, Multivariate process variability monitoring communications in statistics, Theory Methods 37 (2008) 1742–1754.
[19] F.B. Alt, N.D. Smith, Multivariate process control, in: P.R. Krishnaiah, C.R. Rao (Eds.), Handbook of Statistics, Elsevier, 1988, pp. 333–351.
[20] C.L. Yen, J.J.H. Shiau, A multivariate control chart for detecting increases in process dispersion, Stat. Sin. 20 (2010) 1683–1707.
[21] T.J. Rato, M.S. Reis, Sensitivity enhancing transformations for monitoring the process correlation structure, J. Process Control. 24 (2014) 905–915.
[22] N.F. Thornhill, A. Horch, Advances and new directions in plant-wide disturbance detection and diagnosis, Control Eng. Pract. 15 (2007) 1196–1206.
[23] J. Thambirajah, L. Benabbas, M. Bauer, N.F. Thornhill, Cause-and-effect analysis in chemical processes utilizing XML, plant connectivity and quantitative process history, Comput. Chem. Eng. 33 (2009) 503–512.
[24] H. Jiang, R. Patwardhan, S.L. Shah, Root case diagnosis of plant-wide oscillations using the concept of the adjacency matrix, J. Process Control 19 (2009) 1347–1354.
[25] N.F. Thornhill, J.W. Cox, M.A. Paulonis, Diagnosis of plant-wide oscillation through data-driven analysis and process understanding, Control Eng. Pract. 11 (2003) 1481–1490.
[26] L.H. Chiang, Fault Detection and Diagnosis for Large-scale Systems, University of Illinois, Urbana, Illinois, 2001, Ph.D. Thesis.
[27] L.H. Chiang, R.D. Braatz, Process monitoring using causal map and multivariate statistics: fault detection and identification, Chemom. Intell. Lab. Syst. 65 (2003) 159–178.

[28] L.H. Chiang, B. Jiang, X. Zhu, D. Huang, R.D. Braatz, Diagnosis of multiple and unknown faults using the causal map and multivariate statistics, J. Process Control 28 (2015) 27–39.
[29] M.S. Sarfraz, O. Hellwich, Z. Riaz, Feature extraction and representation for face recognition, in: M. Oravec (Ed.), Face Recognition, InTech, Croatia, 2010, pp. 1–20.
[30] W.E. Larimore, Canonical variate analysis in control and signal processing, in: T. Katayama, S. Sugimoto (Eds.), Statistical Methods in Control and Signal Processing, Marcel Dekker Inc., New York, 1997, pp. 83–120.
[31] L.H. Chiang, E.L. Russell, R.D. Braatz, Fault Detection and Diagnosis in Industrial Systems, Springer Verlag, London, UK, 2001.
[32] E.L. Russell, L.H. Chiang, R.D. Braatz, Fault detection in industrial processes using canonical variate analysis and dynamic principal component analysis, Chemom. Intell. Lab. Syst. 51 (2000) 81–93.
[33] C.W.J. Granger, Investigating causal relationships by econometric models and cross-spectral methods, Econometrica 37 (1969) 424–438.
[34] A. Raich, A. Çinar, Diagnosis of process disturbances by statistical distance and angle measures, Comput. Chem. Eng. 21 (1997) 661–673.
[35] S.J. Qin, Statistical process monitoring: basics and beyond, J. Chemom. 17 (2003) 480–502.
[36] B.M. Wise, N.B. Gallagher, S.W. Butler, D.D. White, G.G. Barna, A comparison of principal component analysis, multiway principal component analysis, trilinear decomposition and parallel factor analysis for fault detection in a semiconductor etch process, J. Chemom. 13 (1999) 379–396.
[37] Y. Tamada, S. Kim, H. Bannai, S. Imoto, K. Tashiro, S. Kuhara, S. Miyano, Estimating gene networks from gene expression data by combining Bayesian network model with promoter element detection, Bioinformatics 19 (2003) ii227–ii236.
[38] B. Jiang, D. Huang, X. Zhu, F. Yang, R.D. Braatz, Canonical variate analysis-based contributions for fault identification, J. Process Control 26 (2015) 17–25.
[39] X. Zhu, R.D. Braatz, Two-dimensional contribution map for fault identification, IEEE Control Syst. 34 (2014) 72–77.
[40] G. Lee, S. Song, E.S. Yoon, Multiple-fault diagnosis based on system decomposition and dynamic PLS, Ind. Eng. Chem. Res. 42 (2003) 6145–6154.